Expanded View Figures

Figure EV1. Characterization of *c-myc*$^{\omega t/\omega t}$ and *c-myc*$^{\Delta/\Delta}$ cells.

A *c-myc* copy number relative to a reference amplicon on the *Ncl* gene at different time-points after LPS stimulation in *c-myc*$^{\omega t/\omega t}$ and *c-myc*$^{\Delta/\Delta}$ cells, as indicated. $n = 6$ for the t0 and 24 h samples, $n = 4$ for the 48-h and 72-h samples.

B *c-myc* mRNA expression (normalized to *TBP*) at different time-points after LPS stimulation in *c-myc*$^{\omega t/\omega t}$ and *c-myc*$^{\Delta/\Delta}$ cells. $n = 3$.

C Myc protein levels at different time-points after LPS stimulation in *c-myc*$^{\omega t/\omega t}$ and *c-myc*$^{\Delta/\Delta}$ cells, based on quantification of four independent immunoblots (each produced with B-cell lysates obtained from a pool of 3 mice per genotype): a representative blot is shown above the plot. Note that in wild-type cells, *c-myc* mRNA levels peaked 2 h after LPS stimulation [9], while the protein steadily accumulated over time, consistent with post-transcriptional regulation of its synthesis and/or stability [63,64]: as expected, both mRNA and protein accumulation were blunted in *c-myc*$^{\Delta/\Delta}$ cells.

D Myc and IgG ChIP, as indicated, in non-treated (NT) or LPS-treated (2 h) *c-myc*$^{\omega t/\omega t}$ and *c-myc*$^{\Delta/\Delta}$ B-cells. PCR primers in the *AchR* promoter (as a non-bound control) and in *Ncl* intron 1 (as a known Myc target with 5 E-boxes) were used for quantification (% if input) as previously described [39,65]. $n = 3$.

E Quantification of total RNA levels per cell along the LPS time-course in *c-myc*$^{\omega t/\omega t}$ and *c-myc*$^{\Delta/\Delta}$ cells. $n = 3$.

F Percentages of BrdU-positive cells at 0, 12, and 24 h, as indicated. $n = 3$.

G Growth curve of *c-myc*$^{\omega t/\omega t}$ and *c-myc*$^{\Delta/\Delta}$ cells, as indicated. $n = 3$.

H *c-myc*$^{\omega t/\omega t}$ and *c-myc*$^{\Delta/\Delta}$ cells were sorted according to their size and shape (FSC and SSC, respectively) after 24 or 48 h of LPS stimulation: cells with low and high FSC + SSC were defined as resting and activated, respectively, and were purified by FACS sorting prior to qPCR quantification of *c-myc* copy number, alongside unsorted *c-myc*$^{\Delta/\Delta}$ and *c-myc*$^{\omega t/\omega t}$ control samples. Results from a representative experiment are shown. The experiment was repeated twice with similar results.

I Caspase-3/7 activity normalized on cell numbers along the LPS time-course in *c-myc*$^{\omega t/\omega t}$ and *c-myc*$^{\Delta/\Delta}$ cells. $n = 3$.

Data information: In all the bar plots (except panel H), data are presented as mean ± SD. *$P < 0.05$, **$P < 0.01$, ***$P < 0.001$, Student's *t*-test.

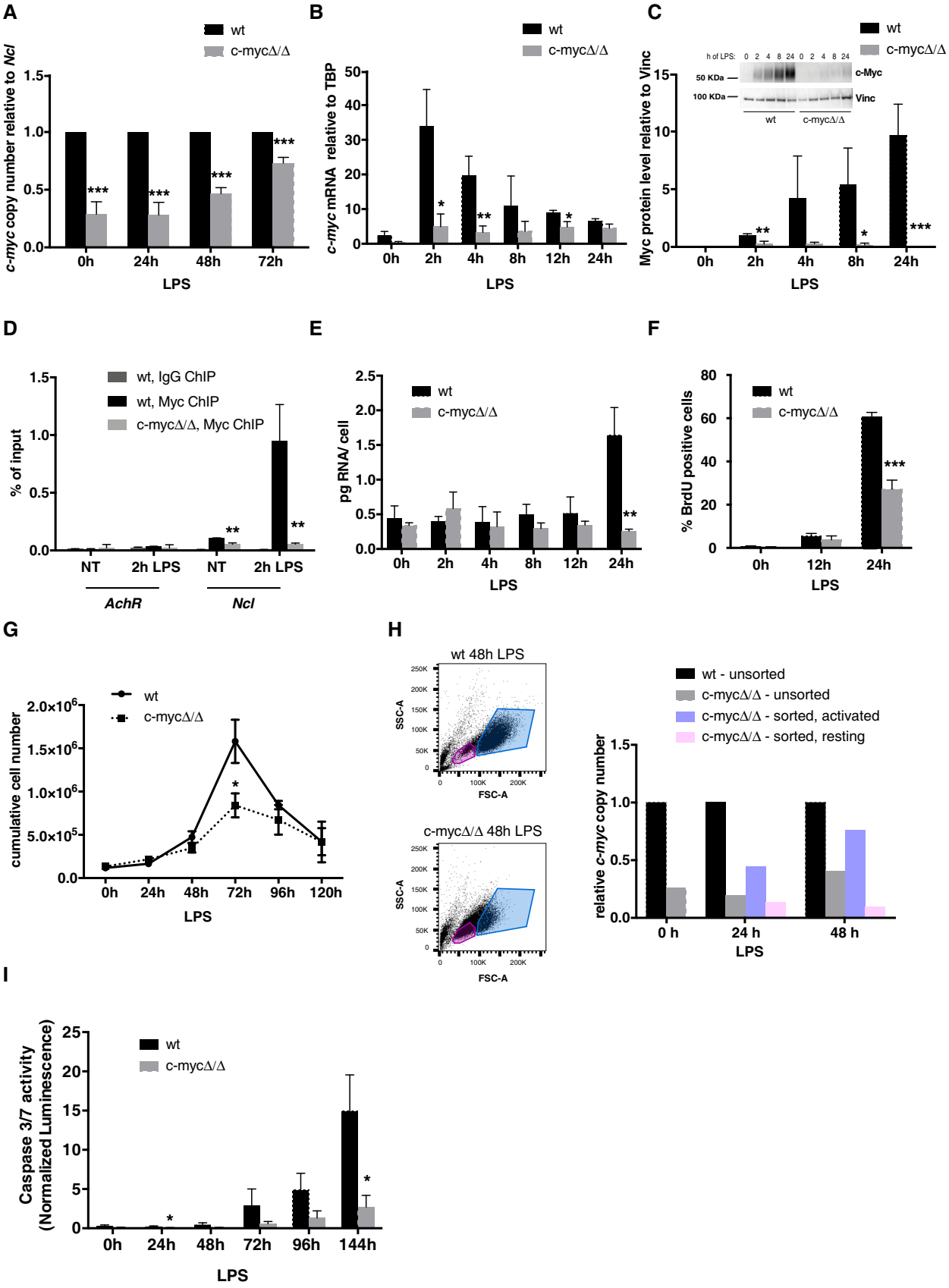

Figure EV1.

A

	class	2h	4h	8h
UP	WT	883	1979	2131
	c-myc Δ/Δ	812	1263	1461
DOWN	WT	874	2157	2187
	c-myc Δ/Δ	1082	1946	1817

B

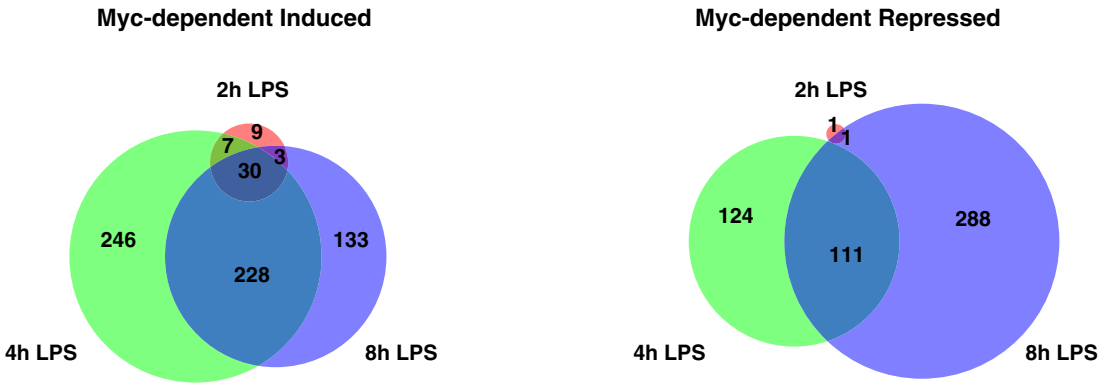

C

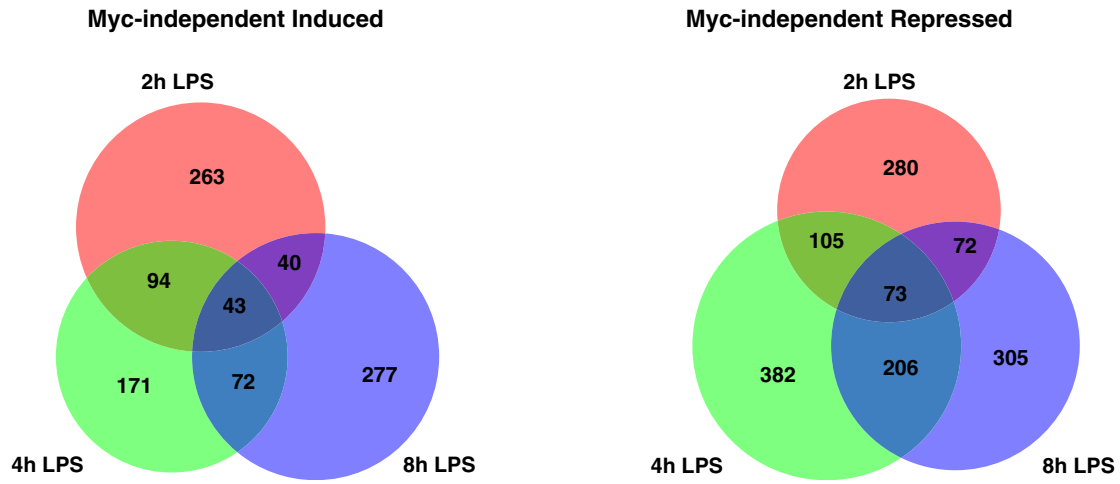

Figure EV2. Time-course analysis of the transcriptional regulatory categories.

A Numbers of genes classified in the different regulatory categories on the basis of the RNA-Seq data at each time-point after LPS stimulation.

B, C Venn diagrams representing the overlap between genes identified as Myc-dependent induced (left) or repressed (right) (B), or Myc-independent LPS-regulated (C), at the different time-points after LPS treatment.

Figure EV3. RNAPII ChIP-Seq data quantification.

A, B Heatmap showing the variations in RNAPII ChIP-Seq read density (log_2FC) in different regions (TSS, gene-body, TES) for Myc-dependent (A) and Myc-independent (B) genes along the LPS time-course, as indicated. The gray scale represents the starting level for each parameter in unstimulated cells. Columns on the left show the changes in Myc share and RNA synthesis rates, as indicated, for the same genes.

C, D Boxplots reporting LPS-induced changes (log_2FC) for each of the four RNAPII kinetic rates in *c-myc*$^{\omega t/\omega t}$ (wt) and *c-myc*$^{\Delta/\Delta}$ cells for Myc-dependent (C) and Myc-independent (D) induced and repressed genes, as indicated. All boxplots are as defined in Fig 2I, and RNAPII replicates as defined in Fig 4B and C.

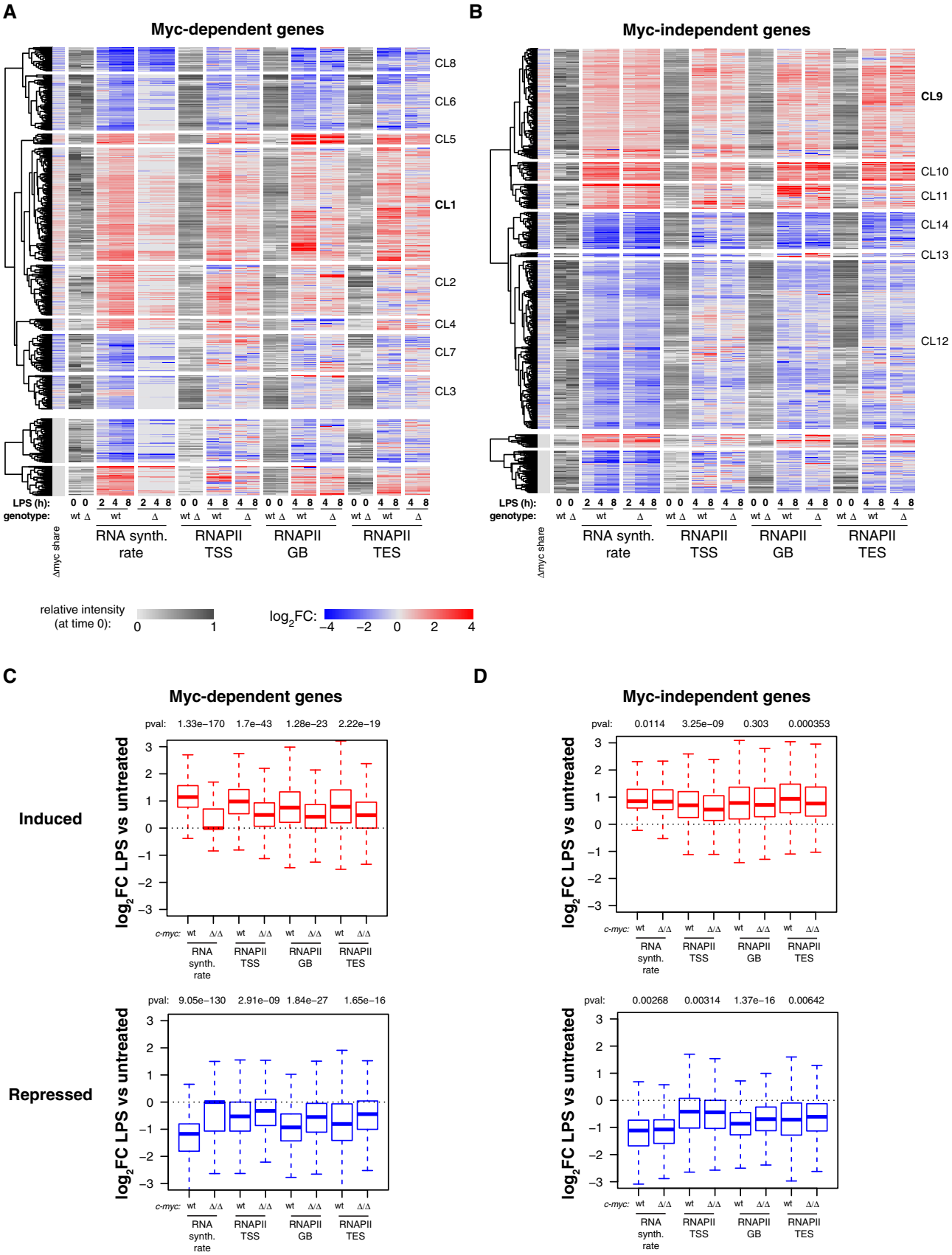

Figure EV3.

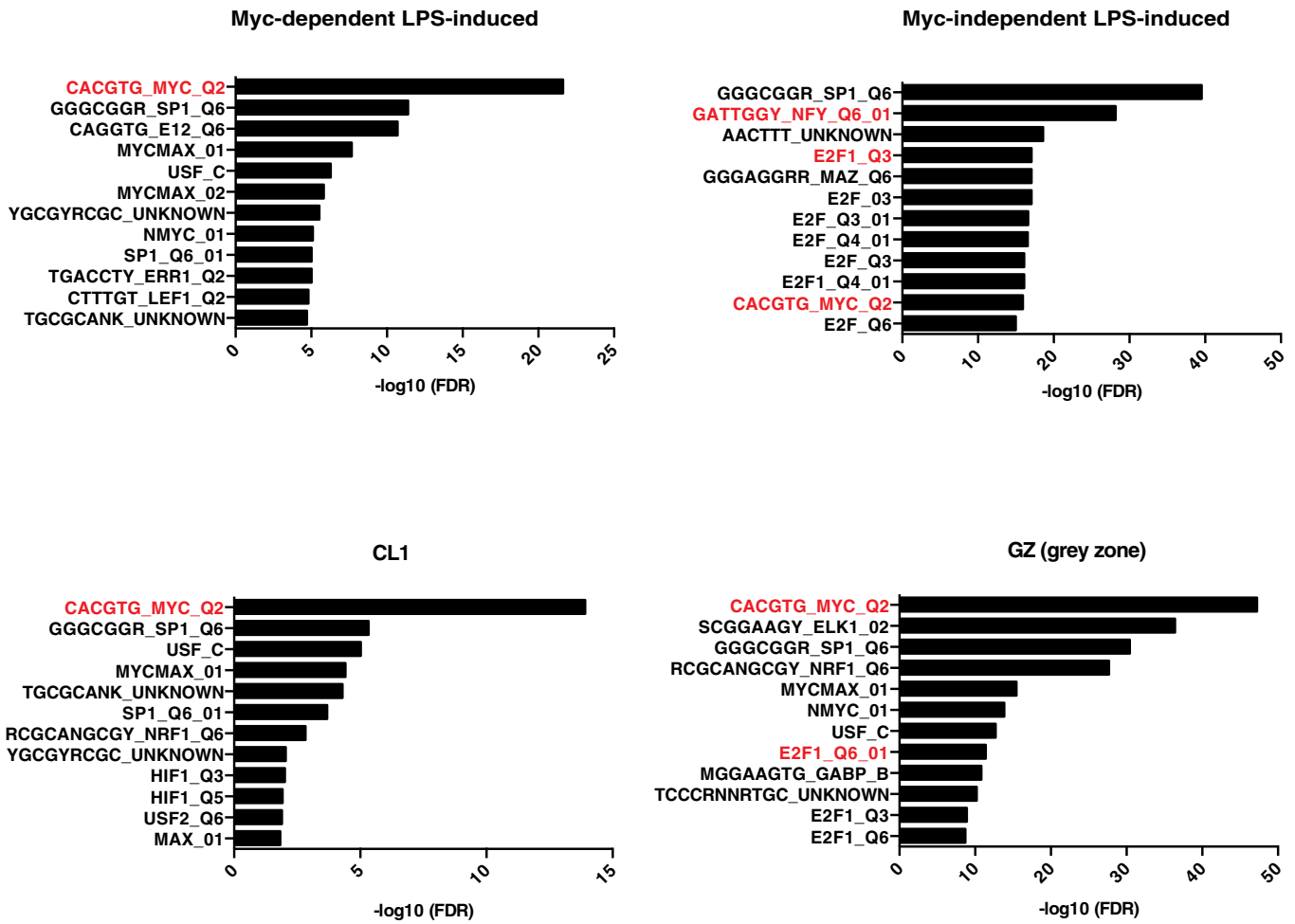

Figure EV4. DNA Motifs analysis of Myc-dependent and Myc-independent LPS-induced genes.
Bar plots showing the −log10 (FDR) of the top 12 cis-regulatory motifs enriched in the promoters of the genes belonging to the indicated regulatory groups.

Figure EV5. Overlap between Myc-dependent LPS-induced genes and other datasets.

A Venn diagrams representing the overlap between Myc-dependent LPS-induced genes defined in this study (either all genes, or only those in CL1) with other lists of Myc-regulated genes. From left to right, and top to bottom: genes less expressed in Myc/Max KO B-cells activated with LPS for 72 h, compared to wt cells [16]; genes more expressed in Myc-positive versus negative germinal center B-cells [10] Myc-dependent serum-responsive (MDSR) genes in fibroblasts [8]; genes down-regulated in Myc-depleted U2OS [29], K562 and HCT116 cells [31].

B Venn diagrams representing the overlap between Myc-dependent LPS-induced genes defined in this study with genes induced in Eμ-*myc* B-cells at the pre-tumoral (left) or tumoral stage (right).

Data information: The *P*-value of the overlap between Myc-dependent LPS-induced genes and the dataset of interest is shown below each diagram.

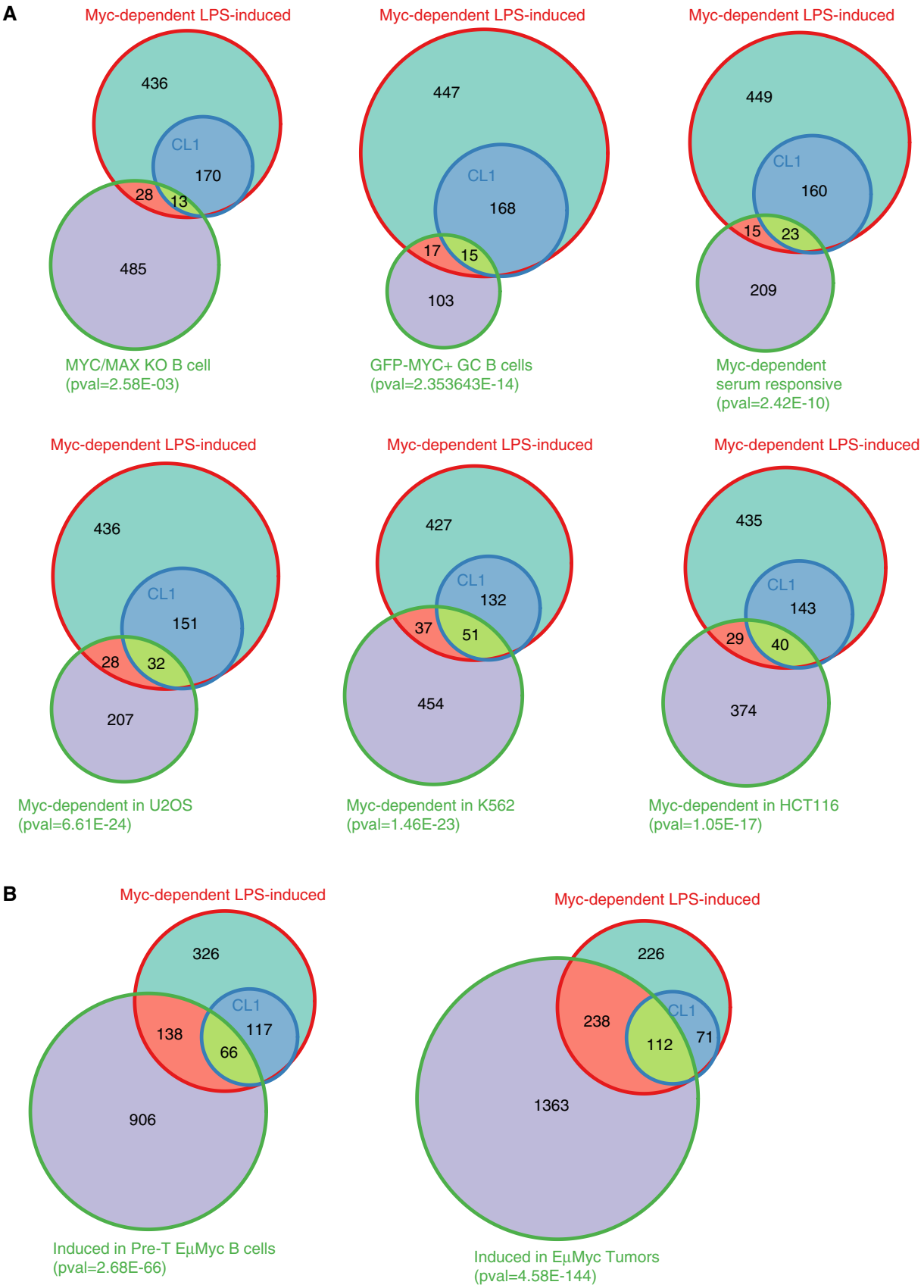

Figure EV5.